Received: 5 January 2021 | Revised: 27 February 2021 | Accepted: 11 March 2021

DOI: 10.1111/bre.12566

RESEARCH ARTICLE

Basin Research IAS EAGE WILEY

Paleo-thermal constraints on the origin of native diagenetic sulfur in the Messinian evaporites: The Northern Apennines foreland basin case study (Italy)

Francesco Paolo Rossi[1] | Andrea Schito[2,3] | Vinicio Manzi[1] | Marco Roveri[1] | Sveva Corrado[2] | Stefano Lugli[4] | Matteo Reghizzi[1]

[1]Department of Chemistry, Life Science and Environmental Sustainability, University of Studying of Parma, Parma, Italy

[2]Department of Science, Geological Sciences Section, University of Studying "Roma Tre", Roma, Italy

[3]Department of Geology and Petroleum Geology, School of Geosciences, University of Aberdeen, Aberdeen, UK

[4]Department of Chemistry and Geological Sciences, University of Studying of Modena and Reggio Emilia, Modena, Italy

Correspondence
Francesco Paolo Rossi, Department of Chemistry, Life Science and Environmental Sustainability, University of Studying of Parma, Parco Area delle Scienze 11/a, 43124, Parma, Italy.
Email: francescopaolo.rossi@studenti.unipr.it

Funding information
University of Roma Tre MIUR (Italian Minister of University and Research) funds for Department of Excellence; University of Parma MIUR funds for Department of Excellence; University of Parma FIL2016-2018 responsible Professor Marco Roveri; University of Parma FIL2016-2018 responsible Professor Vinicio Manzi; MIUR PhD scholarship 2016-2019

Abstract

Recent studies on the genesis of sedimentary native sulfur deposits indicate diagenetic mid-low temperature Bacterial Sulfate Reduction (BSR) as the main process, involving organic compounds (kerogen/hydrocarbons), bacterial colonies and gypsiferous rocks. In the peri-Mediterranean area (Southern Spain, Sicily, Northern Apennines, Israel), the main sulfur accumulations are always associated with late Miocene sulfates and organic-rich successions encompassing the Messinian salinity crisis (MSC). In particular, the Messinian successions of the Apennine-Adriatic foreland basin system, due to a large amount of high-resolution stratigraphic data, represent a perfect case study for understanding the diagenetic conditions controlling the development of the BSR process during sedimentary basin evolution. In this work, thermal models performed in three sub-basins in a sector of the Northern Apennines comprised of the Sillaro and Marecchia rivers (Italy), calibrated by means of organic and inorganic geothermometers, indicate a general thermal immaturity of the studied successions attained as a result of a constant heat flow similar to the present day one (ca. 40 mW/m^2) since Late Tortonian and lithostatic loads between 615 and 1,710 m depending on different sub-basins. These results suggest that the MSC deposits experienced maximum temperatures between about 39°C and 65°C. Temperatures derived from thermal models have been used to constraint occurrence of the diagenetic BSR associated with evaporitic deposits providing thermal constraints in sulfur genesis as well as new useful thermal-constraints for basin analysis studies.

KEYWORDS
Bacterial Sulfate Reduction, gypsum-anhydrite transition, Messinian salinity crisis, sedimentary sulfur, thermal modelling, vitrinite reflectance

1 | INTRODUCTION

Worldwide economically exploited sedimentary native sulfur is mainly associated with large evaporitic deposits. Native sulfur in the Mediterranean area is associated with the Messinian salinity crisis (MSC) evaporites in Italy (Northern Apennines and Sicily), southern Spain (Betic Cordillera) and southern Israel (Caruso et al., 2015; Decima et al., 1988; Dessau et al., 1962; Guido et al., 2007; Krijgsman et al., 1999; Lugli et al., 2013; Manzi et al., 2005, 2011; McKenzie, 1985; Rouchy et al., 1998; Sagui, 1923; Ziegenbalg et al., 2010). Many authors consider the diagenetic Bacterial Sulfate Reduction (BSR; Figure 1) as the main process for the generation of sedimentary sulfur from evaporites in foredeep-foreland geological settings (Davis & Kirkland, 1970; Feely & Kulp, 1957; Manzi et al., 2011; Peckmann et al., 1999; Rouchy et al., 1998; a detailed description of this process is reported in the supplementary information). During BSR native sulfur and associated calcium carbonate (and/or dolomite) are generated involving bacterial colonies, dissolved sulfate rocks (gypsum and anhydrite) and organic compounds and/or hydrocarbons developed by organic matter maturation and/or hydrocarbons migration (Figure 1; Davis & Kirkland, 1970; Feely & Kulp, 1957). Despite extensive isotopic geochemical studies (e.g. Decima et al., 1988; Dessau et al., 1962; Ziegenbalg et al., 2010), the geological conditions necessary to generate BSR-related native sulfur deposits have never been defined in detail. In particular, paleotemperature conditions have been defined only experimentally with no further constraint that can be applied to natural cases (Machel, 2001 and references therein).

The sector of the Northern Apennines comprised between the Sillaro and Marecchia rivers (Italy) is a key area to understand the mechanism and timing of BSR-related sulfur formation that occurred in MSC evaporites in different depositional settings (Figures 2 and 3) of the Apennine-Adriatic foreland basin system. The Vena del Gesso wedge-top marginal basin to the west, where primary shallow-water evaporitic deposits accumulated, is characterised by very limited sulfur occurrence. Conversely, the inner foredeep Romagna sub-basins to the east contain clastic evaporites (turbidites and mass-wasting deposits) and show the largest sulfur deposits in the Apennines.

In this work, we adopted a multidisciplinary approach in order to reconstruct the thermal conditions at which the native sulfur deposition developed, combining thermal data from classical vitrinite analyses with those derived from the gypsum-anhydrite transition. Our findings shed new lights on the temperature and timing conditions necessary to generate diagenetic sulfur that may help similar studies in other worldwide areas.

Highlights

- This work define the diagenetic condition for the sulfur formation in relationship with deposits generated by the Messinian salinity crisis
- This works uses different organic (vitrinite reflectance) and inorganic (gypsum-anhydrite transistion) geothermometers as contraints to define diagenetic conditions for sulfur formation
- Case study are three sub-basins of the Apennine-Adriatic foreland basin system in the Northern Apennines of Italy

2 | THE MESSINIAN SALINITY CRISIS STRATIGRAPHY AND THE BSR SULFUR DEPOSITS

Between 5.97 and 5.33 Ma (Manzi et al., 2013; Van Couvering et al., 2000), the Mediterranean Sea experienced one of the most catastrophic events in its recent geological history, known as the Messinian salinity crisis (MSC; Hsü et al., 1973; Selli, 1973), leading to widespread evaporite

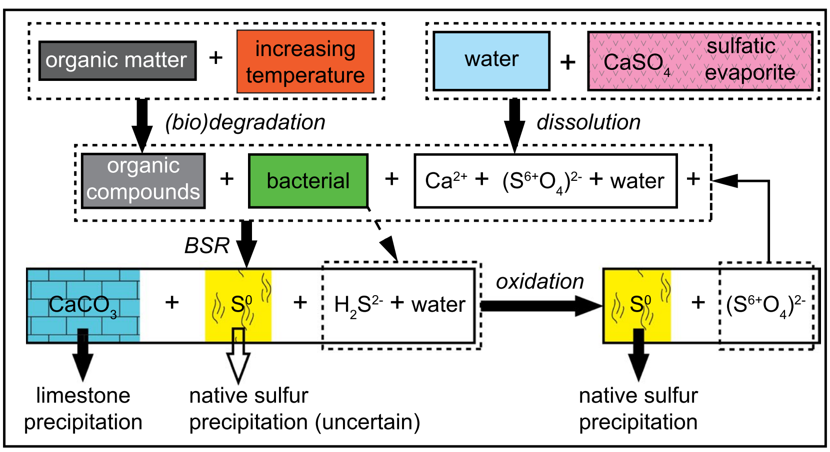

FIGURE 1 Simplified sketch of the diagenetic BSR process. For a complete description see supplementary notes

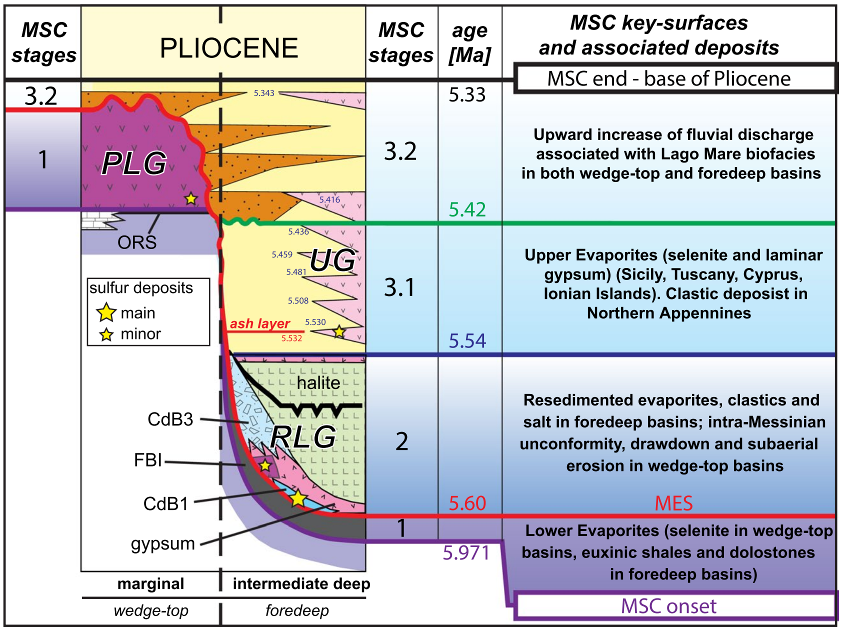

FIGURE 2 MSC deposits correlation panel. CdB1 and CdB3, Calcare di base type 1 and 3 units; FBI, Foraminifera Barren Interval unit; MES, Messinian Erosional Surface. ORS, organic rich shale; PLG, Primary Lower Gypsum unit; RLG, Resedimented Lower Gypsum unit; UG, Upper Gypsum unit; VdG, Vena del Gesso basin. Modified from Manzi et al. (2016)

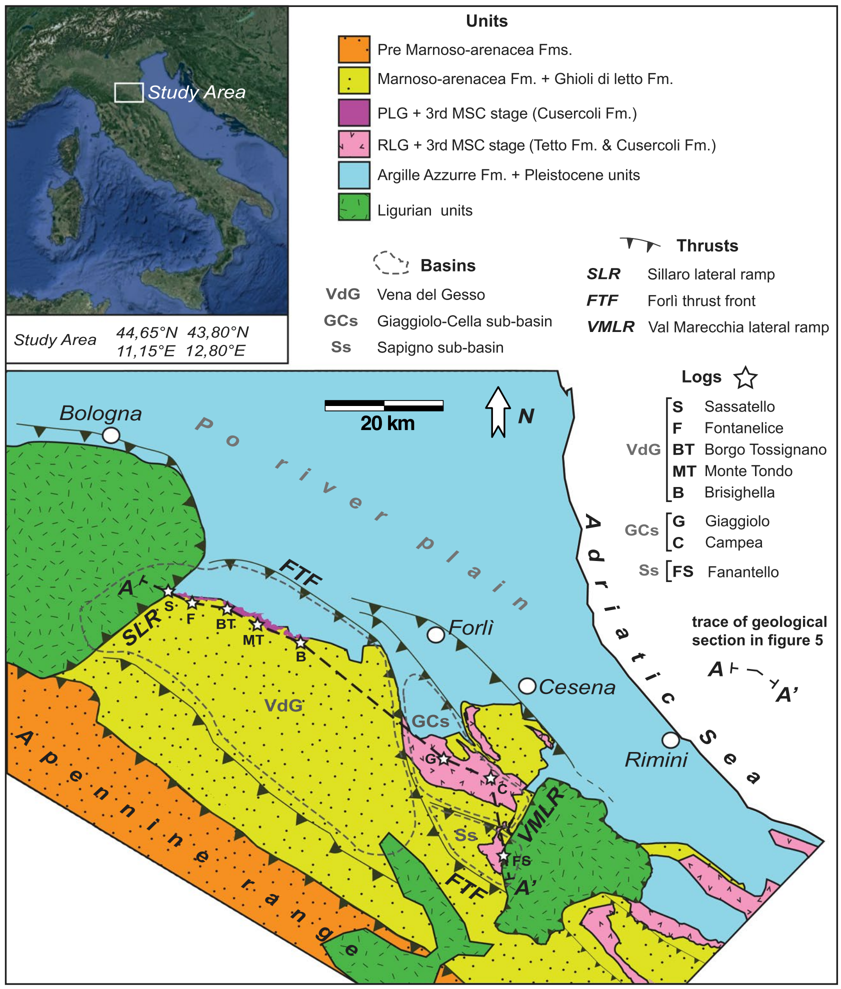

FIGURE 3 Simplified geological map of the study area. Modified from Manzi et al. (2005, 2007)

deposition (Ogniben, 1957; Roveri et al., 2014; Ruggieri, 1967; Selli, 1973 and references therein), through three main stages (CIESM, 2008; Clauzon et al., 1996; Manzi et al., 2012, 2013; Roveri et al., 2009). During the first stage (5.971–5.6 Ma, Figure 2), the marginal basins (paleobathymetry <200 m) experienced the deposition of the Primary Lower Gypsum unit (PLG; De Lange & Krijgsman, 2010; Krijgsman et al., 2001; Lugli et al., 2010; Vai, 1988, 1997;

Vai & Ricci Lucchi, 1977) consisting of decametric-thick selenite beds alternated with decimetric-thick organic-rich muddy interval. Conversely, in the intermediate-deep basins (between 200 and 1,000 m depth, Roveri et al., 2014), organic-rich foraminifera-barren shale with thin dolomite-rich beds (Foraminifera Barren Interval, FBI sensu Manzi et al., 2018) were deposited (Dela Pierre et al., 2011, 2012; Gennari et al., 2013; Lugli et al., 2010; Manzi et al., 2007, 2011). The second stage was the MSC peak (5.6–5.54 Ma, Figure 2; Roveri et al., 2014), with more severe climatic and hydrological conditions recorded by the formation of a tectonic- and/or eustatic-related erosional surface, the Messinian erosional surface (MES, in surface survey, see Roveri et al., 2014 and references therein) or Intra-Messinian unconformity (IMU, in seismic data analysis, see Rossi & Rogledi, 1988; Rossi et al., 2002, 2015; amongst others). This is a regional-scale feature of both subaerial and subaqueous nature depending on the paleo-depth of the basins. As a consequence, the PLG unit of the Vena del Gesso basin was locally exposed, karstified (Costa et al., 1986; De Giuli et al., 1988; Landuzzi & Castellari, 1988; Marabini & Vai, 1988), deeply eroded and resedimented through gravitational processes into the deeper eastern Romagna sub-basins, forming a composite unit with gypsum-bearing turbidites and chaotic deposits (RLG, Resedimented Lower Gypsum, Fortuin & Krijgsman, 2003; Kontopoulos et al., 1997; Lugli et al., 2013; Manzi, 2001; Manzi et al., 2005, 2007, 2011; Omodeo-Salè et al., 2012; Parea & Ricci Lucchi, 1972; Ricci Lucchi, 1973; Robertson et al., 1995; Roveri et al., 2001, 2003; Roveri & Manzi, 2006), which sealed the FBI. Finally, in both marginal and intermediate-deep basins, the third stage (5.54–5.33 Ma, Figure 2) was characterised by more terrigenous successions of sandy-clayey bodies with rhythmic intercalation in its upper portion of conglomerates and micritic limestones (Bassetti et al., 2004; Cita et al., 1978; Orszag-Sperber, 2006; Rouchy & Caruso, 2006; Roveri et al., 1998, 2008; Stoica et al., 2007, 2013; Vasiliev et al., 2004, 2011). In this last stage, primary evaporites (Upper Gypsum, UG) were deposited only in the south-eastern Mediterranean basins (Sicily, Greece, Cyprus). The end of MSC (5.33 Ma, Figure 2) is marked by the abrupt return to open marine conditions and the deposition of open marine sediments in both marginal and intermediate-deep basins (Gennari et al., 2008; Iaccarino et al., 1999; Iaccarino & Bossio, 1999; Roveri et al., 2008). During the post-crisis period (from 5.33 Ma onward, Figure 2), the MSC deposits underwent progressive lithostatic load. Burial-related temperature increase would have set off the BSR process (Ehrlich, 1990; Machel, 1992; Postgate, 1984; Rabus et al., 2006), which is well described by Machel (2001) and resumed in supplementary notes and in Figure 1. The result of this process was the development of native sulfur associated mainly with the clastic deposits of the second stage (Figure 2) as in Sicily (Calcare di base type 1 or CdB1; Manzi et al., 2011 and references therein), locally including PLG olistoliths (Cozzo Disi; Manzi et al., 2016), the Northern Apennines (this work) and Israel (Lugli et al., 2013). Native sulfur developed moderately in stage 1 deposits (Figure 2) of the Northern Apennines (this work) and Spain (Lorca basin, Betic Cordillera, Rouchy et al., 1998). Locally, minor sulfur ore deposits are associated with the UG deposits (Sicily, stage 3, Figure 2, Manzi et al., 2016).

3 | GEOLOGICAL SETTING, STRATIGRAPHY AND EVOLUTION OF THE STUDIED AREA

Our work is focused on three (sub-)basins of the Apennine-Adriatic foreland basin system showing different geological settings (Figures 2 and 3): the marginal Vena del Gesso wedge-top basin (VdG; Roveri et al., 2003 and references therein) and two intermediate-deep inner foredeep basins (Giaggiolo-Cella and Sapigno sub-basins, respectively GCs and Ss; Manzi et al., 2005, 2007; Roveri et al., 1998, 2001, 2003 and references therein). These (sub-)basins are located along the north-eastern flank of the Apennine belt and their tectono-sedimentary evolution was strictly related to the post middle Miocene tectonic events (Rossi et al., 2002, 2015; Roveri et al., 1998, 2001, 2003; Thomson et al., 2010; Zattin et al., 2002), which differently developed in adjacent sectors according to the timing of the local growth of individual morphostructural elements (Ricci Lucchi, 1973, 1981, 1986).

3.1 | Vena del Gesso basin

The VdG basin (Figure 3) was isolated from the main foredeep since the late Tortonian due to the development of a structural high (Forlì thrust front – Riolo anticline; Figure 2; Ricci Lucchi, 1986; Roveri et al., 1998, 2003). This progressive isolation is well recorded in its stratigraphic succession (Figure 4; Krijgsman et al., 1999; Ricci Lucchi, 1986; Ricci Lucchi & Ori, 1985; Roveri et al., 1998, 2003; Vai, 1988, 1997) showing, from base to top: (1) channelised turbidite bodies (Fontanelice Mb.) above the turbiditic lobes of Castel del Rio Mb. (both belonging to the Marnoso-arenacea Fm.), (2) organic-rich shale (ORS; Ghioli di letto Fm. or "euxinic shale", comprising the Tortonian-Messinian boundary at 7.25 Ma) and (3) up to 16 gypsum-shale cycles (PLG unit of Gessoso-solfifera Fm.; Lugli et al., 2010; from 5.971 Ma, Manzi et al., 2013). The PLG is cut on top by the Messinian erosional surface (MES) locally associated with angular discordance (Vai, 1988 amongst others) and sub-aerial exposure in the Monticino quarry (Brisighella area, Figure 2; Costa et al., 1986; De Giuli et al., 1988). During the second stage, the PLG evaporites were eroded and redeposited

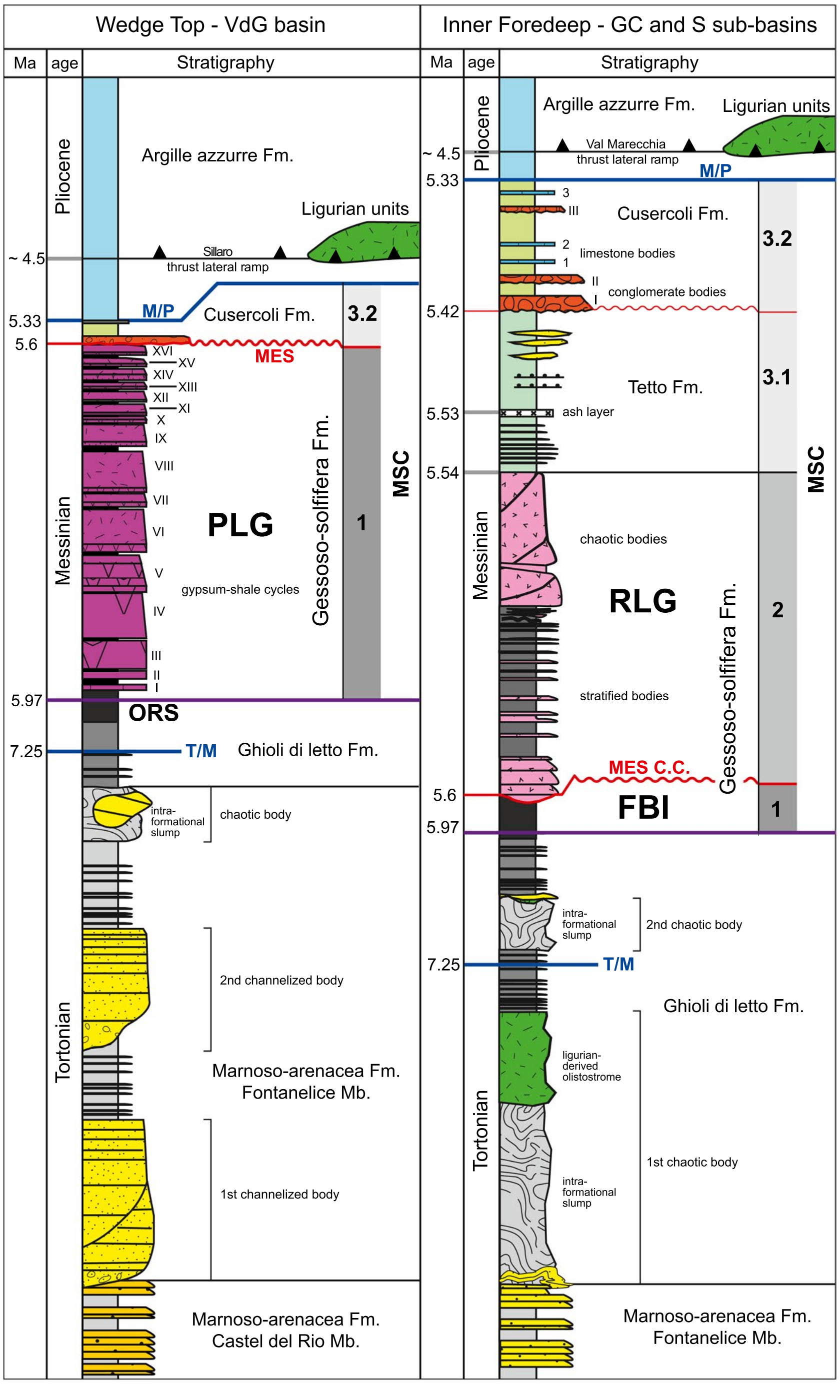

FIGURE 4 Simplified stratigraphy of the three studied (sub-)basins. FBI, Foraminifera Barren Interval unit; GCs, Giaggiolo-Cella sub-basin; MES C.C., Messinian Erosional Surface Correlative Conformity; MES, Messinian Erosional Surface; MSC, Messinian salinity crisis; ORS, organic rich shale; PLG, Primary Lower Gypsum unit; RLG, Resedimented Lower Gypsum unit; Ss, Sapigno sub-basin; T/M, Tortonian-Messinian boundary; VdG, Vena del Gesso basin. Modified from Manzi et al. (2005)

through gravity flows in the adjacent deeper basins. In the Vena del Gesso basin, the whole PLG unit was involved in the sliding (Roveri et al., 2003). The PLG is sealed by clastic deposits (Cusercoli Fm.) that belong to the third stage (5.53–5.33 Ma) and show an extremely reduced thickness (a few tens of metres) accumulated in a time span of about 200 ka; Manzi et al., 2007; Roveri et al., 1998, 2001, 2003; Roveri & Manzi, 2006). Normal marine conditions, suggested by microfossil-rich hemipelagic deposits of the Argille Azzurre Fm., are observed in the basal Zanclean (Pliocene, 5.33 Ma; Hsü et al., 1973; Iaccarino et al., 1999; Manzi et al., 2005; Roveri et al., 2003). This phase is characterised by tectonic quiescence lasting till the MPL3-MPL4 biozones boundary (4 Ma) after which a new tectonic phase, related to Apennines deep-rooted movements, caused the north-eastward tilting of the whole Apennine belt (Roveri et al., 2003; Thomson et al., 2010; Zattin et al., 2002). The sedimentation remained dominated by hemipelagic settling until the middle Pleistocene (0.781 Ma), when the onset of coastal deposits took place (Sabbie di Imola Fm.; Colalongo et al., 1982; Cremonini et al., 1969). The tectonic emplacement of the Ligurian unit (Landuzzi, 1994), heralded by submarine landslides (Val Sellustra Olistostrome Fm.; CARG, 1988), including calcareous olistoliths in a shaley matrix (Castellarin & Pini, 1989), occurred between ca. 4.5 Ma and 0.781 Ma (CARG, 1988; Colalongo et al., 1982) only in the westernmost portion of the VdG basin. Since 4.0 Ma the whole VdG basin was continuously uplifted up to today (Roveri et al., 2003; Thomson et al., 2010; Zattin et al., 2002). The described geological history of the area is simplified in order to provide an overall description of the accumulation/loss of burdening sediment, and thus, the overall increase/decrease of load (temperature); please see Roveri et al. (2003, 2014), Rossi and Rogledi (1988), Rossi et al. (2002, 2015) and references therein for further details. In this area, evidence of gypsum-anhydrite transformation in the PLG unit are generally lacking except in its westernmost portion, close to the Sillaro thrust lateral ramp of the Ligurian nappe. Here, native sulfur is present in small quantities (Figures 4 and 5).

3.2 | Giaggiolo-Cella and Sapigno sub-basins

The GCs and Ss sub-basins (Figures 3–5) are separated from the VdG basin by the Forlì thrust front – Riolo anticline (FTF in Figure 3) and represent an inner foredeep depositional setting (Manzi et al., 2005; Roveri et al., 2001, 2003). Both sub-basins share a similar stratigraphy (Figure 4). Starting from the late Tortonian, the succession is characterised by the turbiditic lobes of the Marnoso-arenacea Fm. (Fontanelice Mb.), followed by thin-bedded turbidites including submarine slides (Ghioli di letto Fm.; Lucente et al., 2002; Manzi et al., 2005, 2007; Roveri et al., 1998, 2001, 2003). The upper portion of this Formation is composed by a 60 m-thick interval of organic-rich shale encompassing the Tortonian-Messinian boundary (7.24 Ma) and the entire early Messinian. The MSC onset (5.971 Ma, Manzi et al., 2013) occurs in the uppermost part of this unit and is marked by the disappearance of foraminifera. This is the Foraminifera Barren Interval unit (FBI; Manzi et al., 2018; Gessoso-solfifera Fm.) representing the deep-water time equivalent of the PLG evaporites (Figures 2 and 4) with scattered or concentrated dolomite and a significant organic matter content (TOC up to 5%; Manzi et al., 2007; Roveri et al., 2016) indicative of strong anoxia and water stratification (Gennari et al., 2013). The FBI unit is sharply overlain by clastic resedimented evaporites composed of gypsum-bearing turbidites and olistostromes deriving from the dismantlement of the PLG unit (RLG unit, Resedimented Lower Gypsum; Gessoso-solfifera Fm.; Manzi, 2001; Manzi et al., 2005, 2007; Parea & Ricci Lucchi, 1972; Ricci Lucchi, 1973; Roveri et al., 2001, 2003; see also Schlager & Bolz, 1977). The RLG unit shows its maximum thickness in the Ss sub-basin (Manzi, 2001; Manzi et al., 2005, 2007) and is floored by an unconformity surface (MES) or its correlative conformity (MES-CC). The succession of the third stage (5.54–5.33 Ma, Bassetti, 2000; Bassetti et al., 1994; Roveri et al., 1998, 2001, 2003), is characterised by a greater thickness (up to 700 m) with respect to that of the VdG and can be subdivided into two Formations (Roveri et al., 1998, 2001, 2003), separated by a minor unconformity. The first formation (Tetto Fm., 5.54–5.42 Ma) is composed of a succession of monotonous shales, interrupted by rare sandstone horizons, and containing a thin volcanoclastic horizon dated at 5.53 Ma (Cosentino et al., 2013; Odin et al., 1997). Differently, the overlying Cusercoli Fm. (5.42–5.33 Ma) is characterised by the alternation of 3 coarse- (conglomerate and pebbly-sandstone fluvio deltaic bodies) and fine-grained (shale and fine sandstone shelf deposits) couplets. Three lacustrine limestone beds (Colombacci) and two paleosoils are also present and the fauna is represented by the typical fresh-water paratethian species found in the

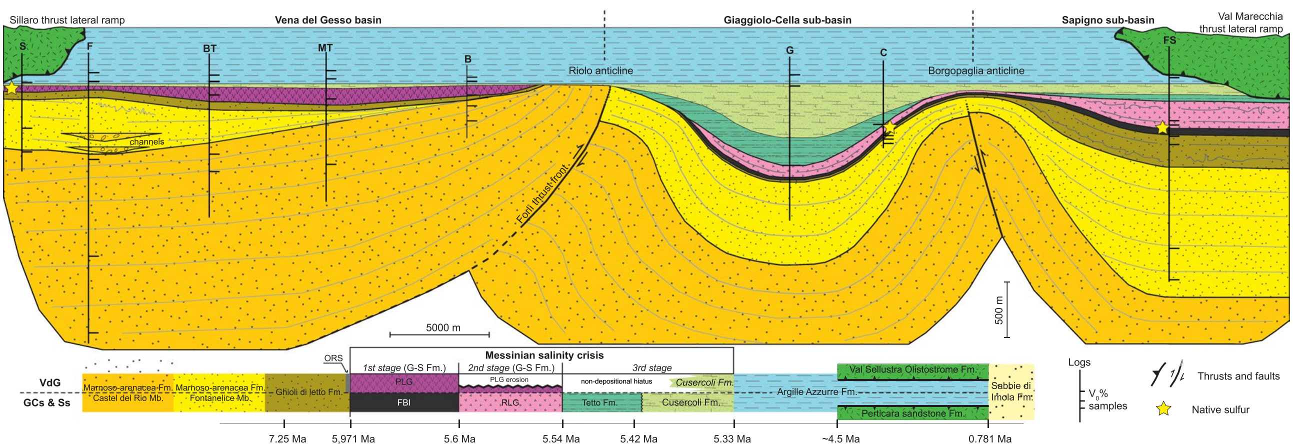

FIGURE 5 Geological section A-A' of Figure 3 with relative chronostratigraphy, position of measured log and organic-rich horizons sampled for R_0% measurement. B, Brisighella log; BT, Borgo Tossignano log; C, Campea log; F, Fontanelice log; FBI, Foraminifera Barren Interval unit; FS, Fanantello log; G, Giaggiolo log; GCs, Giaggiolo-Cella sub-basin; G-S Fm., Gessoso-solfifera Fm; MSC, Messinian salinity crisis; MT, Monte Tondo log; ORS, organic rich shale; PLG, Primary Lower Gypsum unit; R_0%, Vitrinite Reflectance; RLG, Resedimented Lower Gypsum unit; S, Sassatello log; Ss, Sapigno sub-basin; VdG, Vena del Gesso basin

Lago-Mare interval (see Bassetti et al., 2004). As in the VdG basin, the return of normal marine conditions at 5.33 Ma is marked by hemipelagic sediments (Argille Azzurre Fm.) that continued in the GCs sub-basin until the Middle Pleistocene (0.781 Ma). Conversely, in the Ss sub-basin the deposition was interrupted by the emplacement of the Ligurian sheet (Val Marecchia thrust lateral ramp; Elter & Trevisan, 1973; Merla, 1951), capped by the sandy-conglomeratic fluvio-deltaic episutural deposit of the Perticara Sandstone Fm. (De Feyter, 1991; Manzi, 2001; Manzi et al., 2005, 2007; Zattin et al., 2002). The Ss sub-basin loading by the Ligurian units ended in the Middle Pleistocene (0.781 Ma). Since about 4.0 Ma both the Ss and GCs sub-basins experienced a phase of general uplift affecting the whole Northern Apennine mountain range and were subaerially exposed since the Middle Pleistocene (0.781 Ma; Roveri et al., 2003; Thomson et al., 2010; Zattin et al., 2002; for further details). In the two sub-basins, gypsum was transformed into anhydrite during burial and was rehydrated back to gypsum after exhumation by meteoric waters.

4 | MATERIALS AND METHODS

In the VdG basin, we reconstructed five stratigraphic logs spanning from the Late Tortonian to the Pliocene and located in shallowing paleo-settings from the west to the east, progressively closer to the Riolo paleo-high (Figures 3 and 5): Sassatello (S), Fontanelice (F), Borgo Tossignano (BT), Monte Tondo (MT) and Brisighella (B). In the GCs sub-basin, we measured two stratigraphic logs at Giaggiolo (G) and Campea (C) (Figures 3 and 5), including a succession spanning from the Late Tortonian to the Pliocene and located, respectively, in a depocentral area and in a paleo-structural high (Figure 5). In the Ss sub-basin, we measured a single section along the Fanantello stream (FS, Figures 3 and 5) spanning from the Late Tortonian to the Pliocene and located in the core of a syncline dipping south-eastward below the Ligurian Sheet units.

A total of 41 organic-rich fine sediments (shales and marls) samples have been collected: 27 derived from the VdG, six from the GCs and eight from the Ss sub-basins (Figure 5). For each sample, we carried out vitrinite reflectance analyses following the standard methods for sample preparation and measurement (Bustin et al., 1990; Corrado et al., 2019; Lucca et al., 2018; Schito et al., 2016). Results are summarised in Table 1, Figure S1 and Table S3. The eight stratigraphic sections have been modelled using the software BasinMod2D® (Platte River Associates, Inc) based on Sweeney and Burnham's (1990) kinetics model. A general overview on the Vitrinite Reflectance method and Thermal Modelling methods, as well as more information on model inputs are described in the supplementary notes (please see also Figure S2).

TABLE 1 R_0% values and samples location

Log (sub-basin)	Sample name	Location (WGS84) Longitude (°N)	Latitude (°E)	R_0%	Log (sub-basin)	Sample name	Location (WGS84) Longitude (°N)	Latitude (°E)	R_0%
S (VdG)	S18-080	44,22	11,45	0.28 ± 0.04	B (VdG)	B17-040	44,21	11,75	0.26 ± 0.06
	S18-110	44,26	11,47	0.28 ± 0.05		B17-060	44,22	11,76	0.25 ± 0.05
	S18-180	44,28	11,51	0.32 ± 0.05		B17-190	44,23	11,76	0.25 ± 0.05
F (VdG)	F17-030	44,22	11,50	0.37 ± 0.06	G (GCs)	G17-180	44,03	12,06	0.28 ± 0.05
	F17-040	44,24	11,51	031 ± 0.05		G17-210	44,08	11,99	0.24 ± 0.08
	F17-070	44,26	11,56	0.38 ± 0.06	C (GCs)	C17-060	44,06	12,11	0.29 ± 0.07
	F17-180	44,28	11,57	0.24 ± 0.04		C17-090	44,05	12,09	0.30 ± 0.06
	F17-200	44,28	11,54	0.31 ± 0.06		C17-100	44,05	12,09	0.30 ± 0.05
BT (VdG)	BT17-040	44,24	11,59	0.30 ± 0.05		C17-120	44,05	12,09	0.28 ± 0.04
	BT17-070	44,25	11,61	0.29 ± 0.05	FS (Ss)	F17-010	43,91	12,12	0.47 ± 0.05
	BT17-180	44,27	11,63	0.20 ± 0.04		F17-030	43,91	12,13	0.46 ± 0.06
	BT17-190	44,27	11,63	0.14 ± 0.06		F17-075	43,90	12,17	0.36 ± 0.03
MT (VdG)	MT17-040	44,24	11,66	0.25 ± 0.04		F17-085	43,90	12,18	0.31 ± 0.04
	MT17-060	44,24	11,67	0.26 ± 0.05		F17-100	43,90	12,18	0.28 ± 0.06
	MT17-180	44,25	11,68	0.22 ± 0.06		F17-180	43,91	12,22	0.28 ± 0.05

Note: Vitrinite reflectance analysis results.

Abbreviations: B, Brisighella log; BT, Borgo Tossignano log; C, Campea log; F, Fontanelice log; FS, Fanantello log; G, Giaggiolo log; GCs, Giaggiolo-Cella sub-basin; MT, Monte Tondo log; R_0%, Vitrinite Reflectance values and relative errors; S, Sassatello log; Ss, Sapigno sub-basin; VdG, Vena del Gesso basin.

4.1 | Thermal model

The main inputs for thermal models are chronostratigraphy, thermal maturity data (R_0% and $T_{gat,}$ see sup. Materials for a detailed description of these methods) and present-day Heat flow.

Chronostratigraphy (Figure 5; Tables S1 and S2) is mainly based on fieldwork and has been integrated with bibliographic data (Bassetti et al., 1994; Benini et al., 1991; Bassetti, 2000; Capozzi et al., 1991; CARG, 1988; Colalongo et al., 1982; Cremonini et al., 1969; De Feyter, 1991; Farabegoli et al., 1991; Iaccarino et al., 1999; Krijgsman et al., 1999; Lugli et al., 2010; Manzi, 2001; Manzi et al., 2005, 2007, 2013; Odin et al., 1997; Ricchi Lucchi, 1975, 1981, 1986; Ricci Lucchi & Ori, 1985, Roveri et al., 1998, 2001, 2003; Savelli & Wezel, 1978; Vai, 1988, 1997; Van Couvering et al., 2000; Zattin et al., 2002), where lithologies, thicknesses, age and type of bounding surfaces for the portion of the succession preserved from erosion after the Apennines uplift since about 4.0 Ma are reported.

For thermal maturity calibration, vitrinite reflectance data were used. Moreover, the presence or not of re-hydrated gypsum that experienced gypsum-anhydrite transformation was used as a further temperature constraint for the base of evaporitic successions. As matter of fact, petrographic data suggest that gypsum in the western part of VgG basin and in Sapigno and Giaggiolo basins was turned into anhydrite and then re-hydrated back to microcrystalline gypsum (alabastrine) at surface exposure by meteoric waters (Murray, 1964). The presence/absence of alabastrine gypsum allows to define if the original evaporite deposit were/were not heated over the transition temperature, which has been experimentally determined at 51.9°C (Jaworska, 2012; Jowett et al., 1993; Klimchouk, 1996; Murray, 1964).

Assumptions used to run modelling are: (a) decompaction of the burial curves according to Sclater and Christie (1980); (b) thrusting duration is considered instantaneous (Endignoux et al., 1990); (c) a sediment-water-interface temperature of 11°C. Please see Figure S2 for further information.

5 | RESULTS

5.1 | Organic petrography

Thirty-one samples show mean R_0% values comprised between 0.20 and 0.47 (immature stage of HC generation) in all the analysed basins. Most of the samples are rich in the organic matter except some levels of the Argille Azzurre Fm and in the upper part of the Fontanelice Mb. (see Figure S1). In general, from 20 to 50 measurements were carried out on each samples. Vitrinite is the most common maceral and generally shows a small dimension (<10 μm) and different shapes varying from elongated to stocky and from square to slightly rounded. The fragments preservation state is good, although oxidation can occur. Shaly lithologies such as Argille Azzurre or some levels in the Ligurian Units show a high content in amorphous organic matter (AOM), while inertinite is found amongst all over the samples. Reworked organic matter with higher reflectance values was also recognised (blue bars in histograms in Figure S1). Sulfur crystals and sulfides, in particular rhombohedral pyrite, are widespread. Vitrinite reflectance values tend to increase towards the deepest portion (Marnoso-arenacea Fm. samples) in all eight logs.

5.2 | Thermal model calibration

In the VdG basin (F, BT, MT and B logs), thermal model calibration curves match the measured thermal maturity data using a constant heat flow (HF) value of 40 mW/m^2 and an amount of eroded burial of Argille Azzurre Fm. estimated at around 500 m (Figure 6). In all tested scenarios, the temperatures reached by the gypsum and related ORS units are never higher than 44°C (see Table 2).

The S log represents the westernmost area of the VdG basin. Here, thermal model calibration can fit R_0% and T_{gat} constraints, with a constant heat flow of 40 mW/m^2 and an eroded burial of about 1,100 m belonging almost exclusively to the Val Sellustra unit of the Ligurian thrust sheet (Figure 6). Paleotemperatures for the PLG and ORS units overtook T_{gat} (53–55°C) and endured above it for minimum of 20 ka (see Table 2).

In the GCs sub-basin (G and C logs), thermal model calibration is validated using an HF of 40 mW/m^2 and an eroded burial (Argille Azzurre Fm.) of about 470 m (Figure 6). Paleo-temperatures for the RLG unit rests above T_{gat} for minimum of 60 ka showing values within 54°C and 64°C, while the FBI unit reached the maximum temperature of 65°C (see Table 2). Native sulfur deposits developed along the north-eastern flank of the basin (Borgopaglia anticline; Figure 5).

For log FS (Ss sub-basin), its thermal calibration matches measured R_0% and T_{gat} constraints with a constant heat flow of 40 mW/m^2 and an eroded burial of about 1,200 m belonging to Ligurian and Epiligurian units (Figure 6). Paleotemperatures resided above T_{gat} but for a minimum of 110 Ka, maximum temperature reached by the FBI and RLG units is 65°C and 57°C, respectively (see Table 2). Extensive native sulfur generates alongside the north-eastern flank of the sub-basin (sulfiferous limestone).

6 | DISCUSSION

R_0% values (Table 1; Figure S1 and Table S3) point out a general thermal immaturity of the organic matter of the studied

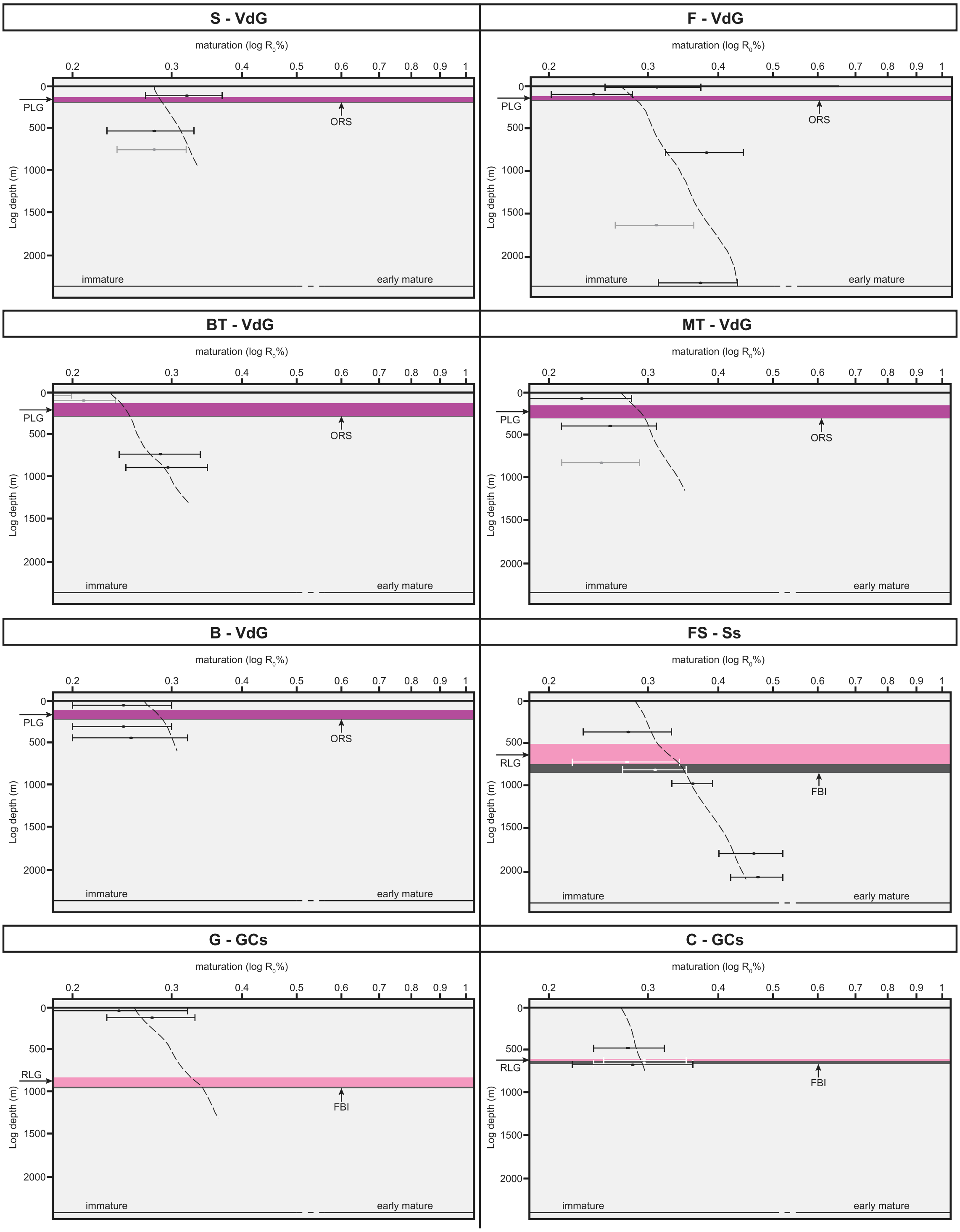

FIGURE 6 Thermal models' calibration by means of vitrinite reflectance data and standard deviations. The pink horizons indicate evaporitic deposits with the FBI and ORS at the base (black horizons). Dotted line indicates calculated thermal maturity across sections using a constant HF of 35 mW/m^2 and different burial loading (see results section for more details). Horizontal lines represent R_0% values (considered in modelling = black or white, not considered in modelling = grey). B, Brisighella log; BT, Borgo Tossignano log; C, Campea log; F, Fontanelice log; FBI, Foraminifera Barren Interval unit; FS, Fanantello log; G, Giaggiolo log; GCS, Giaggiolo-Cella sub-basin; MT, Monte Tondo log; ORS shale, organic rich shale; PLG, Primary Lower Gypsum unit; R_0%, Vitrinite Reflectance; RLG, Resedimented Lower Gypsum unit; S, Sassatello log; SS, Sapigno sub-basin. VdG = Vena del Gesso basin. Immature – Early Mature limit at R_0 = 0.5% to 0.55%

TABLE 2 Modelling results

Basin type	Basin name	Log	Gy-Anh transition	Sulfur	Eroded Fm. or unit	Heat flow (mW/m^2)	Post evaporitic succession, preserved + eroded (m)	Time $T_{gy} > T_{gat}$ (ka)	Paleo-temperatures (°C) Base PLG	Top PLG	Base FBI	FBI-RLG bond	Top RLG
Wedge-top	VdG	S	Yes	Yes	Ligurian sheet	40	110 + 1,100	20	55	53	N.D. a	N.D. a	N.D. a
		F	No	No	Argille Azzurre		120 + 500	N.D. a	40	39	N.D. a	N.D. a	N.D. a
		BT					130 + 500	N.D. a	43	39	N.D. a	N.D. a	N.D. a
		MT					145 + 500	N.D. a	44	39	N.D. a	N.D. a	N.D. a
		B					115 + 500	N.D. a	41	39	N.D. a	N.D. a	N.D. a
Inner foredeep	GCs	G	Yes	Yes			830 + 470	270	N.D. a	N.D. a	65	64	60
		C					610 + 470	60	N.D. a	N.D. a	56	55	54
	Ss	FS			Ligurian sheet		510 + 1,200	110	N.D. a	N.D. a	65	63	57

Note: Results of thermal modelling calibration using HF=40 mW/m^2. "Preserved" may include Tetto, Cusercoli, Argille Azzurre Fm.s and Ligurian sheet unit depending on log (see Table S1); "eroded" includes Argille Azzurre Fm. or Ligurian sheet unit (see Table S1).

Abbreviations: B, Brisighella log; BT, Borgo Tossignano log; C, Campea log; F, Fontanelice log; FBI, Foraminifera Barren Interval unit; FS, Fanantello log; G, Giaggiolo log; GCs, Giaggiolo-Cella sub-basin; MT, Monte Tondo log; N.D. a, value(s) not determinable; PLG, Primary Lower Gypsum unit; RLG, Resedimented Lower Gypsum unit; S, Sassatello log; Ss, Sapigno sub-basin; T_{gat}, Temperature of gypsum-anhydrite transition; T_{gy}, gypsum unit temperature; VdG, Vena del Gesso basin.

successions (pre-oil window $R_0 < 0.50\%–0.55\%$; Hunt, 1995; ICCP, 1971; Stach et al., 1982; Taylor et al., 1998).

Using these data in thermal model calibration we considered possible solutions provided by the interplay between HF and eroded burial variation for all the studied sections (Figure 6), reaching the conclusions that a constant HF from late Tortonian to present day of 40 mW/m^2 for the whole area is the most reliable solution since it best fits with the geological history of the area. This value agrees with the extrapolation of Della Vedova et al. (1995, 2001), with the surface heat flow maps of Italy proposed by CNR in 1994 and is further confirmed by a more recent study by Pauselli et al. (2019) based on new available thermal data from 174 wells in the Northern Apennine. Using such HF values, calculated the thicknesses of eroded burial of both Ligurian and Argille Azzurre units are quite consistent amongst all sections. In detail, calculated thicknesses of overthrusted Ligurian units' range between 1,100 m in the Sassatello section to 1,200 m in the Fanantello (Ss) ones. These values are consistent with Corrado et al. (2010) and Thomson et al. (2010), that, in the same area, found that the AHe (Apatite-Helium geothermometers) system has been not reset and surface Ro% data are generally lower than 0.5% implying surface sediments did not experience temperatures higher than about 60°C–80°C. As well as the reconstruction of the total thicknesses of Argille Azzurre Fm. before erosion never exceed 600m that corresponds to the maximum present-day thicknesses measured in the nearby areas by Conti et al. (2016).

According to thermal models, temperatures experienced by FBI/ORS at the base of the evaporite units in the Ss, GCs and westernmost portion of the VdG (sub-)basins experienced temperatures between 55°C and 65°C (Figure 7), being enough to start organic matter biodegradation (i.e. maturation according to Bjørlykke, 2010; Tissot & Welte, 1984) and, consequently, to develop organic compounds necessary for the BSR process (Machel, 2001 and references therein). Conversely, in the VdG basin where sulfur did not develope, all tested scenarios indicate that the temperatures reached by the ORS were never higher than 44°C.

These results suggest that native sulfur can form from bacterial reduction in sedimentary basins for temperatures higher than 55°C and not lower than 44°C. Notably, the sulfur found in the Perticara Mine (Ss sub-basin) is probably related to the presence of migrated oil deriving from deposits buried in the depocenter of the sub-basin as suggested by Roveri et al. (2016), thus, not only dependent on maximum temperatures recorded in the FS succession.

Likewise, the gypsum-anhydrite transformation developed in high burial condition, thus when temperatures were higher than 53°C (GCs, Ss and western VdG sub-basins) and it never occurs below 44°C (central and eastern VdG basin).

The temperature boundaries of the gypsum-anhydrite transformation have been usually derived from experimental

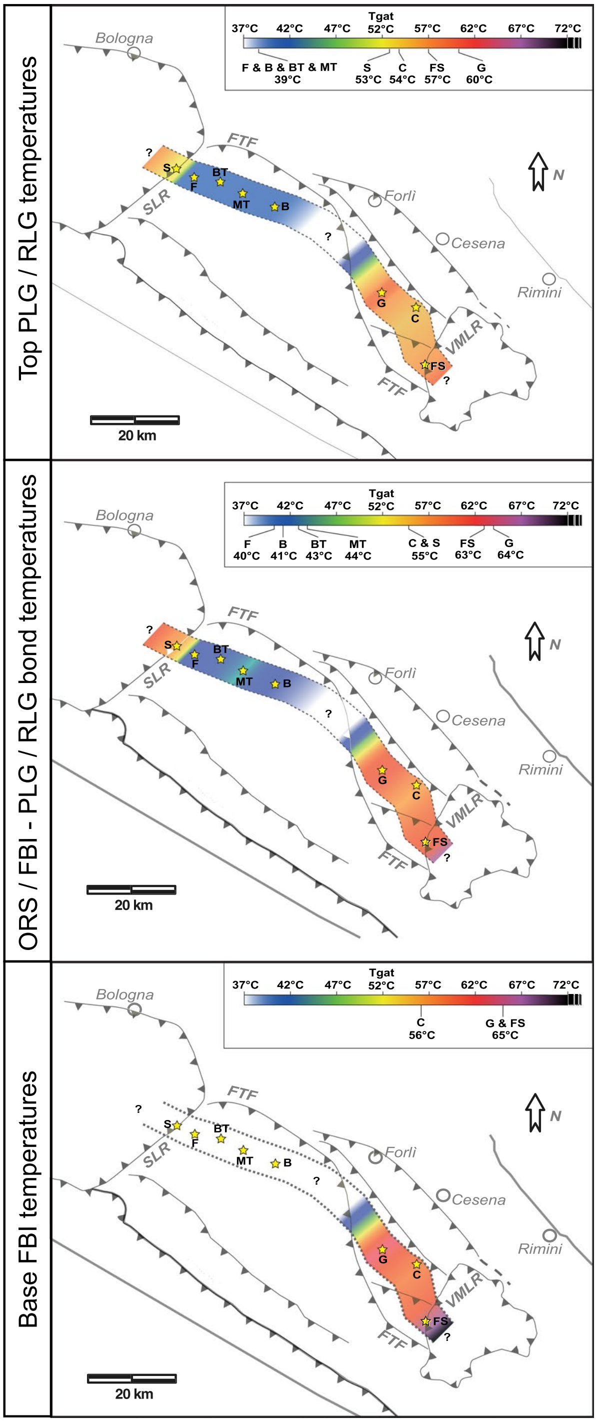

FIGURE 7 Temperatures evolution across different sections studied in this work based on the simplified structural map (cf. with the simplified geological map of Figure 3) with temperatures indicated in Table 2

works while little constraints regarding its occurrence in geological environment are available. According to Jowett et al. (1993), Hardie (1967) and Bredehoeft and Hanshaw (1968), the transition is mainly driven by temperature and by the activity of water. In the presence of coeval NaCl precipitation, the transition occurs at temperatures of 18°C. Nevertheless, according to Jowett et al. (1993), if there is no evidence of salt precipitation and the surrounding lithologies are siliciclastic (sandstone or shales) it can be assumed that pore water reflects the original formation water. The activity of water at which gypsum precipitates is 0.93 and assuming such a number the transition occurs at 51.9°C according to Hardies's (1967) experimental data. In our work, through temperature assessment at the base of the evaporitic successions by mean of the thermal model, we found that in this case history gypsum-anhydrite transition never occurred below 53°C thus in agreement with Jowett et al. (1993) observations. Moreover, we can set a lower limit suggesting that in similar geologic condition (e.g. lithologies and fluids composition), the transition never occurs below 44°C. We also suggest that in a geological environment, the process seems to be very rapid but not strictly time-dependent since it occurred in a time span ranging from 20 to 270 ka.

The gypsum-anhydrite transition released a significant amount of crystallisation water, which may carry significant amounts of dissolved sulfate in contact with the most mature organic-rich shale interfaces, enhancing the BSR process in the Ss, GCs and westernmost portion of the VdG (sub-)basins. Thus, in this work, we suggest a genetic model for sulfur by BSR process in a diagenetic environment that involve the gypsum-anhydrite transformation from original gypsum facies (primary, PLG, or clastic, RLG) and the presence of slight immature organic matter in a temperature window from around 44°C to about 80°C. The lower boundary is suggested by the absence of sulfur in the eastern part of the VdG basin, while the upper limit is the temperature above which sulfate-reducers bacteria do not survive (Jorgensen et al., 2019; Machel, 2001). The association between gypsiferous rocks, presence of organic matter and native sulfur generation was already suggested in the literature by many authors (please see Ziegenbalg et al., 2010; and references therein) on the base of isotopic data. Nevertheless, the great novelty of this work is that we constraint the temperature range in which the process occurs in a natural case history.

The defined temperature window for the BSR-related sulfur genesis may be used for basin analysis purposes, where sulfur of sedimentary origin is present, thus in the other peri-Mediterranean basins and in other worldwide settings containing evaporites. Moreover, the evidence that gypsum-anhydrite transformation and BSR native sulfur formation took place in the same areas is noted even if a certain relationship amongst these two processes cannot be definitely stated here: further analyses are needed to clarify the relationships of the sulfur genesis with the primary gypsum facies and the supposed temperature-related sulfate transition.

Furthermore, from a geological point of view, the results obtained by the reconstruction of the burial and exhumation history of the three (sub-)basins seem in contrast with the idea of a possible paleo-continuity amongst the Sillaro and Val Marecchia tectonic structures as proposed by some authors (see Zattin et al., 2002). Conversely, it can be confirmed the hypothesis that the Ligurian sheet did not develop as a single thrust front, but its allochthonous Northeast-ward movement was hindered by the innermost thrusts involving the oldest portion of the Marnoso-arenacea clastic fill between the Sillaro and Marecchia valleys (Lucente et al., 2002).

7 | CONCLUSIONS

Paleo-thermal data obtained from the thermal modelling of three (sub-)basins of the Northern Apennines provided qualitative and quantitative information on the triggering conditions needed to form native sulfur from evaporites through BSR in both local and regional contexts. A heat flow of 40 mW/m^2 active since the late Tortonian, coupled with a variable lithostatic load produced by about 1,080 to 1,710 m of sediments, generated paleo-temperatures compatible with BSR from 55°C to 64°C at the ORS/FBI and PLG/RLG interfaces. Moreover, considering the minimum paleo-temperature (55°C) reached by the ORS/FBI interface, where native sulfur developed (Giaggiolo-Cella, Sapigno and westernmost portion of Vena del Gesso sub-basins), these conditions are enough for organic matter degradation and generation of organic compounds necessary for BSR. A paleo-temperature slightly lower than 44°C has been reached by the ORS interval underlying the evaporitic unit in the area where sulfur deposits did not develop (eastern Vena del Gesso basin), suggesting that this may be the lower limit for BSR. The evaporites that generated native sulfur also underwent the gypsum-anhydrite transformation, and thus remained over the transition temperature (52°C) for minimum of 20 ka, as shown in the S log example. Hence, the process of anhydritisation appears to be very fast and can release crystallisation water that may provide a significant amount of dissolved sulfate, facilitating the BSR. In summary, the association of BSR-related native sulfur, organic matter maturation and secondary (alabastrine after anhydrite) gypsum deposits define a specific temperature window between about 44°C and 80°C. This temperature interval may be used as paleo-temperatures constraints in the thermal modelling of basins where evaporite and organic-rich sediments were involved in burial-exhumations processes (foredeep-foreland system development). Finally, thermal modelling results obtained in this work also strengthens the idea that both Sillaro and Val Marecchia tectonic elements may be correctly considered as thrust lateral ramps, thus, Ligurian thrust sheet did not develop as a single front.

ACKNOWLEDGEMENTS

This work has benefited from the equipment and framework of the COMP-HUB Initiative (University of Parma), funded by the Department of Excellence programme of the Italian Ministry for Education, University and Research (MIUR, 2018-2022). This work has benefited from University of Roma Tre MIUR funds for the Department of Excellence. This work has benefited from the University of Parma FIL2016-2018 responsible Professor Marco Roveri, University of Parma FIL2016-2018 responsible Professor Vinicio Manzi, MIUR PhD scholarship 2016-2019. Platte River Associates, Inc is kindly acknowledged for providing BasinMod2D® software for research purposes. Massimo Rossi (ENI S.p.A., Milano, Italy) is kindly acknowledged for his review of the manuscript.

PEER REVIEW

The peer review history for this article is available at https://publons.com/publon/10.1111/bre.12566.

DATA AVAILABILITY STATEMENT

The data that support the findings of this study are available from the corresponding author upon reasonable request.

ORCID

Francesco Paolo Rossi https://orcid.org/0000-0002-7999-5404
Andrea Schito https://orcid.org/0000-0003-0760-9321
Vinicio Manzi https://orcid.org/0000-0002-6946-9750
Marco Roveri https://orcid.org/0000-0001-9047-2025
Sveva Corrado https://orcid.org/0000-0001-9727-9973
Stefano Lugli https://orcid.org/0000-0003-1394-4409
Matteo Reghizzi https://orcid.org/0000-0001-8589-096X

REFERENCES

Bassetti, M. A. (2000). Stratigraphy, sedimentology and paleogeography of upper Messinian ('post-evaporitic') deposits in the Marche area (Apennines, central Italy). *Memorie di Scienze Geologiche*, *52*, 319–349.

Bassetti, M. A., Manzi, V., Lugli, S., Roveri, M., Longinelli, A., Ricci Lucchi, F., & Barbieri, M. (2004). Paleoenvironmental significance of Messinian post-evaporitic lacustrine carbonates in the northern Apennines, Italy. *Sedimentary Geology*, *172*, 1–18. https://doi.org/10.1016/j.sedgeo.2004.07.004

Bassetti, M. A., Ricci Lucchi, F., & Roveri, M. (1994). Physical stratigraphy of the Messinian post-evaporitic deposits in the central-southern Marche area (Apennines, central Italy). *Memorie della Societa` Geologica Italiana*, *48*, 275–288.

Benini, A., Farabegoli, E., & Martelli, L. (1991). Stratigrafia e paleogeografia del Gruppo di S. Sofia (alto Appennino Forlivese). *Memorie Descrittive della Carta Geologica d'Italia*, *46*, 231–243.

Bjørlykke, K. (2010). *Petroleum geoscience, from sedimentary environments to rock physics* (p. 508). Springer-Verlag, Berlin Heidelberg.

Bredehoeft, J. D., & Hanshaw, B. B. (1968). On the maintenance of anomalous fluid pressure: I. Thick Sedimentary Sequences. *GSA Bulletin*, *79*. https://doi.org/10.1130/0016-7606(1968)79[1097:OTMOAF]2.0.CO;2

Bustin, R. M., Barnes, M. A., & Barnes, W. C. (1990). Determining levels of organic diagenesis in sediments and fossil fuels. In *Diagenesis, geoscience* (pp. 205-226). Canada Reprint, 4th series.

Capozzi, R., Landuzzi, A., Negri, A., & Vai, G. B. (1991). Stili deformativi ed evoluzione tettonica della successione neogenica romagnola: Studi Geologici Camerti. special, no. 1, 261–278.

CARG project. (1988). CARtografia Geologica.

Caruso, A., Pierre, C., Blanc-Valleron, M.-M., & Rouchy, J. M. (2015). Carbonate deposition and diagenesis in evaporitic environments: The evaporative and sulphur-bearing limestones during the settlement of the Messinian salinity crisis in Sicily and Calabria. *Palaeogeography, Palaeoclimatology, Palaeoecology*, *429*, 136–162. https://doi.org/10.1016/j.palaeo.2015.03.035

Castellarin, A., & Pini, G. A. (1989). L'arco del Sillaro: La messa in posto delle ''Argille Scagliose'' al margine appenninico padano (Appennino bolognese). *Memorie della Società Geologica Italiana*, *39*, 127–141.

CIESM. (2008). The Messinian salinity crisis from mega-deposits to microbiology – A consensus report. CIESM Workshop Monographs, 33 F. Braind Ed., (p. 168), Monaco.

Cita, M. B., Ryan, W. B. F., & Kidd, R. B. (1978). Sedimentation rates in Neogene deep-sea sediments from the Mediterranean and geodynamic implications of their changes. *Deep Sea Drilling Project Initial Reports*, *42*, 1978. https://doi.org/10.2973/dsdp.proc.42-1.152.1978

Clauzon, G., Suc, J. P., Gautier, F., Berger, A., & Loutre, M. F. (1996). Alternate interpretation of the Messinian salinity crisis: Controversy resolved? *Geology*, *24*, 363–366. https://doi.org/10.1130/0091-7613(1996)024<0363:AIOTMS>2.3.CO;2

CNR. (1994). Surface heat flow density map of Italy. Atlas of Geothermal Resources in Europe. CNR, Italy – Updating 1994.

Colalongo, M. L., Ricci Lucchi, F., Guarnieri, P., & Mancini, E. (1982). Il Plio-Pleistocene del Santerno (Appennino romagnolo). In G. Cremonini & F. Ricci Lucchi (Eds.), *Guida alla geologia del margine appenninico padano*. Guide Geologiche regionali della Società Geologica Italiana: Bologna, Società Geologica Italiana, 161–166.

Conti, S., Fioroni, C., Fontana, D., & Grillenzoni, C. (2016). Depositional hystory of the Epiligurian wedge-top basin in the Val Marecchia area (northern Apenines, Italy): A revision of the Burdigalian-tortonian succession. *Italian Journal of Geosciences*, *135*(2), 324–335. https://doi.org/10.3301/IJG.2015.32

Corrado, S., Aldega, L., Perri, F., Critelli, S., Muto, F., Schito, A., & Tripodi, V. (2019). Detecting syn-orogenic extension and sediment provenance of the Cilento wedge top basin (southern Apennines, Italy): Mineralogy and geochemistry of fine-grained sediments and petrography of dispersed organic matter. *Tectonophysics*, *750*, 404–418. https://doi.org/10.1016/j.tecto.2018.10.027

Corrado, S., Aldega, L., & Zattin, M. (2010). Sedimentary vs. tectonic burial and exhumation along the Apennines (Italy). In M. Beltrando, A. Peccerillo, M. Mattei, S. Conticelli, & C. Doglioni (Eds.), *The Geology of Italy: Tectonics and life along plate margins*, Journal of the Virtual Explorer, *36*, 15. https://doi.org/10.3809/jvirtex.2010.00232

Costa, G. P., Colalongo, M. L., De Giuli, C., Marabini, S., Masini, F., Torre, D., & Vai, G. B. (1986). Latest Messinian vertebrate fauna preserved in a paleokarst neptunian dike setting (Brisighella, Northern Apennines). *Le grotte d'Italia*, *12*, 221–235.

Cosentino, D., Buchwaldt, R., Sampalmieri, G., Iadanza, A., Cipollari, P., Schildgen, T. F., Hinnov, L. A., Ramezani, J., & Bowring, S. A. (2013). Refining the Mediterranean "Messinian gap" with high-precision U-Pb zircon geochronology, central and northern Italy. *Geology*, *41*, 323–326. https://doi.org/10.1130/G33820.1

Cremonini, G., Elmi, C., & Monesi, A. (1969). Osservazioni geologiche e sedimentologiche su alcune sezioni plio-pleistoceniche dell'Appennino romagnolo. *Giornale di Geologia*, *35*, 85–96.

Davis, J. B., & Kirkland, D. W. (1970). Native sulfur deposition in the Castile Formation, Culberson County, Texas. *Economic Geology*, *65*, 107–121. https://doi.org/10.2113/gsecongeo.65.2.107

De Feyter, A. J. (1991). Gravity tectonics and sedimentation of the Montefeltro, Italy. *Geologica Ultraiectina*, *35*, 7–168.

De Giuli, C., Masini, F., & Torre, D. (1988). The mammal fauna of the Monticino quarry. In C. De Giuli & G. B. Vai (Eds.), *Fossil vertebrates in the Lamone valley, Romagna Apennines, International Workshop: Continental Faunas at the Mio-Pliocene Boundary* (pp. 28–31). Field Trip Guidebook, Gaenza Litografica, 65–69.

De Lange, G. J., & Krijgsman, W. (2010). Messinian salinity crisis: A novel unifying shallow gypsum/deep dolomite formation mechanism. *Marine Geology*, *275*, 273–277. https://doi.org/10.1016/j.margeo.2010.05.003

Decima, A., McKenzie, J. A., & Schreiber, B. C. (1988). The origin of "evaporative" limestones: An example from the Messinian of Sicily (Italy). *Journal of Sedimentary Petrology*, *58*, 256–272. https://doi.org/10.1306/212F8D6E-2B24-11D7-8648000102C1865D

Dela Pierre, F., Bernardi, E., Cavagna, S., Clari, P., Gennari, R., Irace, A., Lozar, F., Lugli, S., Manzi, V., Natalicchio, M., Roveri, M., & Violanti, D. (2011). The record of the Messinian salinity crisis in the Tertiary Piedmont Basin (NW Italy): The Alba Section revisited. *Palaeogeography, Palaeoclimatology, Palaeoecology*, *310*, 238–255. https://doi.org/10.1016/j.palaeo.2011.07.017

Dela Pierre, F., Clari, P., Bernardi, E., Natalicchio, M., Costa, E., Cavagna, S., Lozar, F., Lugli, S., Manzi, V., Roveri, M., & Violanti, D. (2012). Messinian carbonate-rich beds of the Tertiary Piedmont Basin (NW Italy): Microbially-mediated products straddling the onset of the salinity crisis. *Palaeogeography, Palaeoclimatology, Palaeoecology*, *344–345*, 78–93. https://doi.org/10.1016/j.palaeo.2012.05.022

Della Vedova, B., Bellani, S., Pellis, G., & Squarci, P. (2001). Deep temperature and surface heat flow distribution. In G. B. Vai & I. Peter Martini (Eds.), *Anatomy of an Orogen. The Apennines and Adjacent Mediterranean Basins. Chapter: Chapter 7 – Deep temperatures and surface heat flow distribution*. Kluwer Academic Publisher. https://doi.org/10.1007/978-94-015-9829-3_7

Della Vedova, B., Lucazeau, F., Pasquale, V., Pellis, G., & Verdoya, M. (1995). Heat-flow in the tectonic provinces crossed by the southern segment of the European geotraverse. *Tectonophysics*, *244*(1–3), 57–74. https://doi.org/10.1016/0040-1951(94)00217-W

Dessau, G., Jensen, M. L., & Nakai, N. (1962). Geology and isotopic studies of Sicilian sulfur deposits. *Economic Geology*, *57*, 410–438. https://doi.org/10.2113/gsecongeo.57.3.410

Ehrlich, H. L. (1990). *Geomicrobiology*, (2nd ed, p. 646). Marcel Dekker.

Elter, P., & Trevisan, L. (1973). Alistostromes in the tectonic evolution of the Norther Apennines. In K. A. DeJong & S. Robert (Eds.), *Gravity and tectonics* (pp. 175–188). John Wiley and Sons.

Endignoux, L., Wolf, S., & Letouzey, J. (1990). Thermal and kinematic evolution of thrust basins: A 2D numerical model. *Petroleum and Tectonics in Mobile Belts: Paris*, *47*, 181–192.

Farabegoli, E., Benini, A., Martelli, L., Onorevoli, G., & Severi, P. (1991). Geologia dell'Appennino Romagnolo da Campigna a Cesenatico. *Memorie Descrittive della Carta Geologica d'Italia*, *46*, 165–184.

Feely, H. W., & Kulp, J. L. (1957). Origin of Gulf coast salt-dome sulphur deposits. *Bulletin of the American Association of Petroleum Geologists*, *41*, 1802–1853. https://doi.org/10.1306/0BDA5939-16BD-11D7-8645000102C1865D

Fortuin, A. R., & Krijgsman, W. (2003). The Messinian of the Nijar Basin (SE Spain): Sedimentation, depositional environments and paleogeographic evolution. *Sedimentary Geology*, *160*, 213–242. https://doi.org/10.1016/S0037-0738(02)00377-9

Gennari, R., Iaccarino, S. M., Di Stefano, A., Sturiale, G., Cipollari, P., Manzi, V., Roveri, M., & Cosentino, D. (2008). The messinian-zanclean boundary in the northern Apennine. *Stratigraphy*, *5*(3–4), 307–322.

Gennari, R., Manzi, V., Angeletti, L., Bertini, A., Biffi, U., Ceregato, A., Faranda, C., Gliozzi, E., Lugli, S., Menichetti, E., Rosso, A., Roveri, M., & Taviani, M. (2013). A shallow water record of the onset of the Messinian salinity crisis in the Adriatic foredeep (Legnagnone section, Northern Apennines). *Palaeogeography, Palaeoclimatology, Palaeoecology*, *386*, 145–164. https://doi.org/10.1016/j.palaeo.2013.05.015

Guido, A., Jacob, J., Gautret, P., Laggoun-Défarge, F., Mastandrea, A., & Russo, F. (2007). Molecular fossils and other organic markers as palaeoenvironmental indicators of the Messinian Calcare di Base Formation: normal versus stressed marine deposition (Rossano Basin, northern Calabria, Italy). *Palaeogeography, Palaeoclimatology, Palaeoecology*, *255*, 265–283. https://doi.org/10.1016/j.palaeo.2007.07.015

Hardie, L. A. (1967). The Gypsum-Anhydrite equilibrium at one atmosphere pressure. *American Mineralogist*, *52*, 171–200.

Hsü, K. J., Cita, M. B., & Ryan, W. B. F. (1973). The origin of the Mediterranean evaporites. In W. B. F. Ryan, K. J. Hsü, P. Dumitrica, J. M. Lort, W. Maync, W. D. Nesteroff, G. Pautot, H. Stradner & F. C. Wezel (Eds.), *Initial reports of the deep sea drilling project*, Vol. *XIII* (pp. 1203–1231). Government Printing Office.

Hunt, J. M. (1995). *Petroleum geochemistry and geology* (p. 743). Freeman.

Iaccarino, S. M., & Bossio, A. (1999). Paleoenvironment of uppermost Messinian sequences in the western Mediterranean (sites 974, 975 and 978). In R. Zahn, M. C. Comas & A. Klaus (Eds.), *Proceedings of the Ocean Drilling Program, Scientific Results* (Vol. *161*, pp. 529–540). Ocean Drilling Program. https://doi.org/10.2973/odp.proc.sr.161.246.1999

Iaccarino, S., Castradori, D., Cita, M. B., Di Stefano, E., Gaboardi, S., McKenzie, J. A., Spezzaferri, S., & Sprovieri, R. (1999). The Miocene/Pliocene boundary and the significance of the earliest Pliocene flooding in the Mediterranean. *Memorie della Società Geologica Italiana*, *54*, 109–131.

International Committee for Coal Petrology (ICCP). (1971). *International Handbook of Coal Petrography, 1st Supplement to* ss CNRS.

Jaworska, J. (2012). Crystallization, alternation and recrystallization of sulphates. In advances in crystallization processes. 1st ed. crystallization, alternation and recrystalization of sulphates. INTECH. Y. Mastai. https://doi.org/10.13140/2.1.4282.4322

Jorgensen, B. B., Findlay, A. J., & Pellerin, A. (2019). The biogeochemical sulfur cycle of marine sediments. *Frontier in Microbiology*, *10*, 549. https://doi.org/10.3389/fmicb.2019.00849

Jowett, E. C., Cathles, L. M. III, & Davis, B. W. (1993). Predicting depths of gypsum dehydration in evaporitic sedimentary basin. *AAPG Bulletin V*, *3*, 402–413. https://doi.org/10.1306/BDFF8C22-1718-11D7-8645000102C1865D

Klimchouk, A. (1996). The dissolution and conversion of gypsum and anhydrite. *International Journal of Speleology*, *25*, 21–36. https://doi.org/10.5038/1827-806X.25.3.2

Kontopoulos, N., Zelilidis, A., Piper, D. J. W., & Mudie, P. J. (1997). Messinian evaporites in Zakynthos, Greece. *Palaeogeography, Palaeoclimatology and Palaeoecology*, *129*, 361–367. https://doi.org/10.1016/S0031-0182(96)00117-4

Krijgsman, W., Fortuin, Ar, Hilgen, Fj, & Sierro, Fj (2001). Astrochronology for the Messinian Sorbas basin (SE Spain) and orbital (precessional) forcing for evaporite cyclicity. *Sedimentary Geology*, *140*(1-2), 43–60. https://doi.org/10.1016/S0037-0738(00)00171-8

Krijgsman, W., Hilgen, F. J., Marabini, S., & Vai, G. B. (1999). New paleomagnetic and cyclostratigraphic age constraints on the Messinian of the Northern Apennines (Vena del Gesso Basin, Italy). *Memorie della Società Geologica Italiana*, *54*, 25–33.

Landuzzi, A. (1994). Relationships between the Marnoso-arenacea Formation of the Inner Romagna units and the Ligurids (Italy). *Memorie della Socieà Geologica Italiana*, *48*, 523–534.

Landuzzi, A., & Castellari, M. (1988). A new vertebrate site from late Messinian karst holes, Santerno Valley, W Romagna. In C. De Giuli & G. B. Vai (Eds.), *Fossil vertebrates in the Lamone valley, Romagna Apennines, International Workshop: Continental Faunas at the Mio-Pliocene Boundary* (pp. 28–31). Field Trip Guidebook, Faenza Litografica, 70-74.

Lucca, A., Storti, F., Molli, G., Muchez, P., Schito, A., Artoni, A., Balsamo, F., Corrado, S., & Mariani, E. S. (2018). Seismically enhanced hydrothermal plume advection through the process zone of the Compione extensional Fault, Northern Apennines, Italy. *Bulletin*, *131*(3–4), 547–571. https://doi.org/10.1130/B32029.1

Lucente, C. C., Manzi, V., Ricci Lucchi, F., & Roveri, M. (2002). Did the Ligurian sheet cover the whole thrust belt in Tuscany and Romagna Appennines? Some evidence from gravity emplaced deposits. *Memorie della Societa` Geologica Italiana, Volume Speciale*, *1*, 393–398.

Lugli, S., Gennari, S., Gvirtzman, Z., Manzi, V., Roveri, M., & Schreiber, C. B. (2013). Evidence of clastic evaporites in the canyons of the Levant Basin (Israel): Implications for the Messinian salinity crisis. *Journal of Sedimentary Research*, *83*, 942–954. https://doi.org/10.2110/jsr.2013.72

Lugli, S., Manzi, V., Roveri, M., & Schreiber, C. B. (2010). The Primary Lower Gypsum in the Mediterranean: A new facies interpretation first stage of the Messinian salinity crisis. *Palaeogeography, Palaeoclimatology, Palaeoecology*, *297*, 83–99. https://doi.org/10.1016/j.palaeo.2010.07.017

Machel, H. G. (1992). Low-temperature and high-temperature origins of elemental sulfur in diagenetic environments. In G. R. Wessel & B. H. Wimberly (Eds.), *Native sulfur – Developments in geology and exploration* (pp. 3-22). Society for Mining, Metallurgy and Exploration, Inc.

Machel, H. G. (2001). Bacterial and thermochemical sulfate reduction in diagenetic settings – old and new insights. *Sedimentary Geology*, *140*, 143–175. https://doi.org/10.1016/S0037-0738(00)00176-7

Manzi, V. (2001). *Stratigrafia fisica, analisi sedimentologica microscopica e caratteri magnetostratigrafici dei depositi connessi all'evento evaporitico del Messiniano (F.ne Gessoso-solfifera)* [Ph.D. thesis], Bologna,Italy, University of Bologna, 1–72.

Manzi, V., Gennari, R., Hilgen, F., Krijgsman, W., Lugli, S., Roveri, M., & Sierro, F. J. (2013). Age refinement of the Messinina salinity crisis onset in the Mediterranean. *Terra Nova*, *25*, 315–322. https://doi.org/10.1111/ter.12038

Manzi, V., Gennari, R., Lugli, S., Persico, D., Reghizzi, M., Roveri, M., Schreiber, B. C., Calvo, R., Gavrieli, I., & Gvirtzman, Z. (2018). The onset of the Messinian salinity crisis in the deep Eastern Mediterranean basin. *Terra Nova*, *30*(3), 189–198. https://doi.org/10.1111/ter.12325

Manzi, V., Gennari, R., Lugli, S., Roveri, M., Scafetta, N., & Schreiber, B. C. (2012). High frequency cyclicity in the Mediterranean Messinian evaporites: evidence for solar-lunar climate forcing. *Journal of Sedimentary Research*, *82*, 991–1005. https://doi.org/10.2110/jsr.2012.81

Manzi, V., Lugli, S., Ricci Lucchi, F., & Roveri, M. (2005). Deep-water clastic evaporites deposition in the Messinian Adriatic foredeep (northern Apennines, Italy): did the Mediterranean ever dry out? *Sedimentology*, *52*, 875–902. https://doi.org/10.1111/j.1365-3091.2005.00722.x

Manzi, V., Lugli, S., Roveri, M., Schreiber, B. C., & Gennari, R. (2011). The Messinian "Calcare di Base" (Sicily, Italy) revisited. *Geological Society of America Bulletin*, *123*, 347–370. https://doi.org/10.1130/B30262.1

Manzi, V., Lugli, S., Roveri, M., Dela Pierre, F., Gennari, R., Lozar, F., Natalicchio, M., Chalotte Schreiber, B., Taviani, M. & Turco, E. (2016). The Messinian Salinity Crisis in Cyprus: A further step toward a new stratigraphic framework for Eastern Mediterranean. *Basin Research*, *28*, 207–236. https://doi.org/10.1111/bre.12107

Manzi, V., Roveri, M., Gennari, R., Bertini, A., Biffi, U., Giunta, S., Iaccarino, S. M., Lanci, L., Lugli, S., Negri, A., Riva, A., Rossi, M. E., & Taviani, M. (2007). The deep-water counterpart of the Messinian Lower Evaporites in the Apennine foredeep: The Fanantello section (Northern Apennines, Italy). *Palaeogeography, Palaeoclimatology, Palaeoecology*, *251*, 470–499. https://doi.org/10.1016/j.palaeo.2007.04.012

Marabini, S., & Vai, G. B. (1988). Geology of the Monticino Quarry (Brisighella, Italy) stratigraphic implication of its late Messinian Mammal Fauna. In C. De Giuli & G. B. Vai (Eds.), *Fossil vertebrates in the Lamone valley, Romagna Apennines, International Workshop: Continental Faunas at the Mio-Pliocene Boundary* (pp. 39–52). Field Trip Guidebook, Faenza Litografica.

McKenzie, J. A. (1985). Stable-isotope mapping in Messinian evaporative carbonates of central Sicily. *Geology*, *13*, 851–854.

Merla, G. (1951). *Geologia dell'Appennino Settentrionale: Bollettino della Società Geologica Italiana*, *70*, 95–382.

Murray, R. C. (1964). Origin and diagenesis of gypsum and anhydrite. *Journal of Sedimentary Petroleum*, *34*, 512–523. https://doi.org/10.1306/74D710D2-2B21-11D7-8648000102C1865D

Odin, G. S., Deino, A., Cosca, M., Laurenzi, M. A., & Montanari, A. (1997). Miocene geochronology: methods, techniques, results. In A. Montanari, G. S. Odin & R. Coccioni (Eds.), *Miocene stratigraphy: an integrated approach* (pp. 583–596). Elsevier. https://doi.org/10.1016/S0920-5446(06)80043-9

Ogniben, L. (1957). Secondary gypsum of the sulphur series, Sicily, and the so-called integration. *Journal of Sedimentary Geology*, *27*, 64–79. https://doi.org/10.1306/74D7065F-2B21-11D7-8648000102C1865D

Omodeo-Sale', S., Gennari, R., Lugli, S., Manzi, V., & Roveri, M. (2012). Tectonic and climatic control on the Late Messininan sedimentary evolution of the Nijar Basin (Betic Cordillera, Southern Spain). *Basin Research*, *24*, 314–337. https://doi.org/10.1111/j.1365-2117.2011.00527.x

Orszag-Sperber, F. (2006). Changing perspectives in the concept of "Lago-Mare" in Mediterranean Late Miocene evolution. *Sedimentary Geology*, *188–189*, 259–277. https://doi.org/10.1016/j.sedgeo.2006.03.008

Parea, G. C., & Ricci Lucchi, F. (1972). Resedimented evaporites in the Periadriatic trough (upper Miocene, Italy). *Israel Journal of Earth-Sciences*, *21*, 125–141.

Pauselli, C., Gola, G., Mancinelli, P., Trumpy, E., Saccone, M., Manzella, A., & Ranalli, G. (2019). A new surface heat flow map of the Northern Apennines between latitudes 42.5 and 44.5 N. *Geothermics*, *81*, 39–52.

Peckmann, J., Paul, J., & Thiel, V. (1999). Bacterially mediated formation of diagenetic aragonite and native sulfur in Zechstein carbonates (Upper Permian, Central Germany). *Sedimentary Geology*, *126*, 205–222. https://doi.org/10.1016/S0037-0738(99)00041-X

Postgate, J. R. (1984). *The sulfate-reducing bacteria* (2nd ed, p. 208). Cambridge University Press.

Rabus, R., Hansen, T. A., & Widdel, F. (2006). Dissimilatory sulfate- and sulfur-reducing prokaryotes. *Prokaryotes*, *2*, 659–768. https://doi.org/10.1007/0-387-30742-7_22

Ricci Lucchi, F. (1973). Resedimented evaporites: Indicators of slope instability and deep-basins conditions in Periadriatic Messinian (Apennines foredeep, Italy). In *Messinian events in the Mediterranean: Koninklijke Nederlandse Akademie van Wetenschappen*, Geodynamics Scientific Report no. 7, 142-149.

Ricci Lucchi, F. (1975). Miocene palaeogeography and basin analysis in the Periadriatic Apennines. In C. Squyres (Ed.), *Geology of Italy* (Vol. *2*, pp. 129–236). P.E.S.L.

Ricci Lucchi, F. (1981). The Miocene Marnoso-arenacea turbidites, Romagna and Umbria Apennines. In Ricci Lucchi, F. (Ed.), *Excursion guidebook: Bologna, Italy, 2nd International Association of Sedimentologists Regional Meeting*, 229–303.

Ricci Lucchi, F. (1986). The Oligocene to Holocene foreland basins of the northern Apennines. In Allen, P.A. & Homewood, P. (Eds.), *Foreland basins: International Association of Sedimentologists Special Publication* 8, 105–139.

Ricci Lucchi, F., & Ori, G. G. (1985). Field excursion D: Syn-orogenic deposits of a migrating basin systems in the northwest Adriatic foreland. In P. A. Allen (Ed.), *Foreland basins, Excursion guidebook: Fribourg* (pp. 137–176). International Association of Sedimentologists.

Robertson, A. H. F., Eaton, S., Follows, E. J., & Payne, A. S. (1995). Depositional processes and basin analysis of Messinian evaporites in Cyprus. *Terra Nova*, *7*, 233–253. https://doi.org/10.1111/j.1365-3121.1995.tb00692.x

Rossi, M., Minervini, M., Ghielmi, M., & Rogledi, S. (2015). Messinian and Pliocene erosional surfaces in the Po Plain-Adriatic Basin: Insights from allostratigraphy and sequenza stratigraphy in assessing play concepts related to accomodation and gateway turnarounds in tectonically margins. *Marine and Petroleum Geology*, *66*(2015), 192–216. https://doi.org/10.1016/j.marpetgeo.2014.12.012

Rossi, M., & Rogledi, S. (1988). Relative sea-level changes, local tectonic setting and basin margin sedimentation in the interference zone between two orogenic belts: seismic stratigraphic examples from Padan foreland basin, northern Italy. In W. Nemec & R. J. Steel (Eds.), *Fan deltas: Sedimentology and tectonic settings* (p. 368–384). Blackie and Son.

Rossi, M., Rogledi, S., Barbacini, G., Casadei, D., Iaccarino, S., & Papani, G. (2002). Tectono-stratigraphic aschitecture of Messinian piggyback basins of Northern Apenines: The Emilia folds in the Reggio-Modena area and comparison with the Lombardia and Romagna sectors. *Bollettino-Societa Geologica Italiana*, *1*, 437–447.

Rouchy, J. M., & Caruso, A. (2006). The Messinian salinity crisis in the Mediterranean Basin: A reassessment of the data and an integrated scenario. *Sedimentary Geology*, *188–189*, 35–67. https://doi.org/10.1016/j.sedgeo.2006.02.005

Rouchy, J. M., Taberner, C., Blanc-Valleron, M. M., Sprovieri, R., Russell, M., Pierre, C., Di Stefano, E., Pueyo, J. J., Caruso, A., Dinares-Turell, J., Gomis-Coll, E., Wolff, G. A., Cespuglio, G., Ditchfielde, P., Pestrea, S., Combourieu-Nebout, N., Santisteban, C., & Grimalt, J. O. (1998). Sedimentary and diagenetic markers of the restriction in a marine basin: the Lorca Basin (SE Spain) during the Messinian. *Sedimentary Geology*, *121*, 23–55. https://doi.org/10.1016/S0037-0738(98)00071-2

Roveri, M., Bassetti, M. A., & Ricci Lucchi, F. (2001). The Mediterranean Messinian salinity crisis: An Apennine foredeep perspective. *Sedimentary Geology*, *140*, 201–214. https://doi.org/10.1016/S0037-0738(00)00183-4

Roveri, M., Bertini, A., Cosentino, D., Di Stefano, A., Gennari, R., Gliozzi, E., Grossi, F., Iaccarino, S. M., Lugli, S., Manzi, V., & Taviani, M. (2008). A high-resolution stratigraphic framework for the latest Messinian events in the Mediterranean area. *Stratigraphy*, *5*, 323–342.

Roveri, M., Gennari, R., Lugli, S., & Manzi, V. (2009). The Terminal Carbonate Complex: the record of sea-level changes during the Messinian salinity crisis. *GeoActa*, *8*, 57–71.

Roveri, M., Gennari, R., Lugli, S., Manzi, V., Minelli, N., Reghizzi, M., Riva, A., Rossi, M. E., & Chreiber, B. C. (2016). The Messinina salinity crisis: open problems and possible implications for Mediterranean petroleum system. *Petroleum Geoscience*, *22*(4), 89. https://doi.org/10.1144/petgeo2015-089

Roveri, M., & Manzi, V. (2006). The Messinian salinity crisis: looking for a new paradygm? *Palaeogeography, Palaeoclimatology, Palaeoecology*, *238*, 386–398. https://doi.org/10.1016/j.palaeo.2006.03.036

Roveri, M., Manzi, V., Bassetti, M. A., Merini, M., & Ricci Lucchi, F. (1998). Stratigraphy of the Messinian post-evaporitic stage in eastern Romagna (northern Apennines, Italy). *Giornale di Geologia*, *60*, 119–142.

Roveri, M., Manzi, V., Ricci Lucchi, F., & Rogledi, S. (2003). Sedimentary and tectonic evolution of the Vena del Gesso Basin (Northern Apennines, Italy): implications for the onset of the Messinian salinity crisis. *Geological Society of America Bulletin*, *115*(4), 387–405. https://doi.org/10.1130/0016-7606(2003)115<0387:SATEOT>2.0.CO;2

Roveri, R., Flecker, R., Krijgsman, W., Lofi, J., Lugli, S., Manzi, V., Sierro, F. J., Bertini, A., Camerlenghi, A., De Lange, G., Govers, R., Hilgen, F. J., Hübscher, C., Meijer, P. T. H., & Stoica, M. (2014). The Messinian salinity crisis: Past and future of a great challenge for marine sciences. *Marine Geology*, *352*, 25–58. https://doi.org/10.1016/j.margeo.2014.02.002

Ruggieri, G. (1967). The Miocene and later evolution of the Mediterranean Sea. In Ager, A. V. & Adams, C. G. (Eds.). *Aspects of Tethyan Biogeography*, *7*, 283-290.

Sagui, C. L. (1923). The sulphur mines of Sicily. *Economic Geology*, *18*.

Savelli, D., & Wezel, F. C. (1978). Schema geologico del Messiniano nel Pesarese. *Bollettino Società Geologica Italiana*, *97*, 165–188.

Schito, A., Corrado, S., Aldega, L., & Grigo, D. (2016). Overcoming pitfalls of vitrinite reflectance measurements in the assessment of thermal maturity: the case history of the lower Congo basin. *Marine and Petroleum Geology*, *74*, 59–70. https://doi.org/10.1016/j.marpetgeo.2016.04.002

Schlager, W., & Bolz, H. (1977). Clastic accumulation of sulphate evaporites in deep water. *Journal of Sedimentary Petrology*, *47*, 600–609. https://doi.org/10.1306/212F71F3-2B24-11D7-8648000102C1865D

Sclater, J. G., & Christie, P. A. F. (1980). Continental stretching: An explanation of the post-mid-Cretaceous subsidence of the central North Sea basin. *Journal of Geophysical Research: Solid Earth*, *85*, 3711–3739.

Selli, R. (1973). *An outline of the Italian Messinian. Koninklijke Nederlandse Akademie Van Wetenshappen: Messinian Events in the Mediterranean Geodynamics*, Scientific Report 7 of the Colloquium held in Utrecht. 150-171

Stach, E., Mackowsky, M. T., Teichmüller, M., Taylor, G. H., Chandra, D., & Teichmuller, R. (1982). *Stach's textbook of coal petrology*. Gebrüder Borntraeger.

Stoica, M., Lazăr, I., Krijgsman, W., Vasiliev, I., Jipa, D., & Floroiu, A. (2013). Paleoenvironmental evolution of the East Carpathian foredeep during the late Miocene-early Pliocene (Dacian Basin; Romania). *Global and Planetary Change*, *103*, 135–148. https://doi.org/10.1016/j.gloplacha.2012.04.004

Stoica, M., Lazar, I., Vasiliev, I., & Krijgsman, W. (2007). Mollusc assemblages of the Pontian and Dacian deposits from the Topolog-Arges area (southern Carpathian foredeep – Romania). *Geobios*, *40*, 391–405. https://doi.org/10.1016/j.geobios.2006.11.004

Sweeney, J. J., & Burnham, A. K. (1990). Evaluation of the Simple Model of Vitrinite Reflectance Base on Chemical Kinetics. *The American Association of Petroleum Geologists Bulletin*, *74*, 1559–1570. https://doi.org/10.1306/0C9B251F-1710-11D7-8645000102C1865D

Taylor, G. H., Teichmuller, M., Davis, A., Diessel, C. F. K., Littke, R., & Robert, P. (1998). *Organic Petrology* (p. 704). Gebrüder Borntraeger.

Thomson, S. N., Brandon, M. T., Reiners, P. W., Zattin, M., Isaacson, P. J., & Balestrieri, M. L. (2010). Thermochronologic evidence for orogen-parallel variability in wedge kinematics during extending convergent orogenesis of the northern Apennines, Italy. *GSA Bulletin*, *122*(7/8), 1160–1179. https://doi.org/10.1130/B26573.1

Tissot, B. P., & Welte, D. H. (1984). *Petroleum formation and occurrence* (2nd ed, p. 699). Springer-Verlag.

Vai, G. B. (1988). The Lamone Valley: a field trip guide to the Romagna Apennines. In C. De Giuli & G. B. Vai (Eds.), *Fossil vertebrates in the Lamone Valley, Romagna Apennines, field trip guide-book International workshop: Continental faunas at the Mio-Pliocene boundary* (pp. 7–37).

Vai, G. B. (1997). Cyclostratigraphic estimate of the Messinian stage duration. In A. Montanari, G. S. Odin & R. Coccioni (Eds.), *Miocene stratigraphy – An integrated approach: Amsterdam* (pp. 463–476). Elsevier.

Vai, G. B., & Ricci Lucchi, F. (1977). Algal crusts autochthonous and clastic gypsum in a cannibalistic evaporite basin: A case history from the Messinian of Northern Apennines. *Sedimentology*, *24*, 211–244.

Van Couvering, J. A., Castradori, D., Cita, M. B., Hilgen, F. J., & Rio, D. (2000). The base of the Zanclean Stage and of the Pliocene Series. *Episodes*, *23*, 179–187. https://doi.org/10.18814/epiiugs/2000/v23i3/005

Vasiliev, I., Iosifidi, A. G., Khramov, A. N., Krijgsman, W., Kuiper, K. F., Langereis, C. G., Popov, V. V., Stoica, M., Tomsha, V. A.,

& Yudin, S. V. (2011). Magnetostratigraphy and radiometric dating of upper Miocene-lower Pliocene sedimentary successions of the Black Sea Basin (Taman Peninsula, Russia). *Palaeogeography, Palaeoclimatology, Palaeoecology*, *310*, 163–175.

Vasiliev, I., Krijgsman, W., Langereis, C. G., Panaiotu, C. E., Matenco, L., & Bertotti, G. (2004). Towards an astrochronological framework for the eastern Paratethys Mio-Pliocene sedimentary sequences of the Focsani basin (Romania). *Earth and Planetary Science Letters*, *227*, 231–247. https://doi.org/10.1016/j.epsl.2004.09.012

Zattin, M., Picotti, V., & Zuffa, G. G. (2002). Fission-track reconstruction of the front of the Northern Apennine thrust wedge and overlying Ligurian unit. *American Journal of Science*, *302*, 346–379. https://doi.org/10.2475/ajs.302.4.346

Ziegenbalg, S. B., Brunner, B., Rouchy, J. M., Birgel, D., Pierre, C., Böttcher, M. E., Caruso, A., Immenhauser, A., & Peckmann, J. (2010). Formation of secondary carbonates and native sulphur in sulphate-rich Messinian strata, Sicily. *Sedimentary Geology*, *227*, 37–50. https://doi.org/10.1016/j.sedgeo.2010.03.007

SUPPORTING INFORMATION

Additional Supporting Information may be found online in the Supporting Information section.

How to cite this article: Rossi FP, Schito A, Manzi V, et al. Paleo-thermal constraints on the origin of native diagenetic sulfur in the Messinian evaporites: The Northern Apennines foreland basin case study (Italy). *Basin Res*. 2021;00:1–17. https://doi.org/10.1111/bre.12566